Electronic Supplementary Information

Microfluidic nozzle device for ultrafine fiber solution blow spinning with precise diameter control[†]

Eddie Hofmann,[a,b] Kilian Krüger,[a,b] Christian Haynl,[c] Thomas Scheibel,[c] Martin Trebbin,[d] Stephan Förster[a,b]

[a] Department of Physical Chemistry I, University of Bayreuth, 95440 Bayreuth, Germany.
[b] Jülich Centre for Neutron Science (JCNS-1/ICS-1), Forschungszentrum Jülich GmbH, 52425 Jülich, Germany.
[c] Department for Biomaterials, University of Bayreuth, 95440 Bayreuth, Germany.
[d] Centre for Ultrafast Imaging (CUI), University of Hamburg, 22761 Hamburg, Germany.

Analyzing the fiber diameter

When analyzing the fiber samples via scanning electron microscopy, the quadratic mean (RMS) and the standard deviation (SD) were determined. For each parameter set, an adequate number n of single fibers was measured. Since later calculations assume volume constancy, the arithmetic mean of the fiber volume (Eq. S2) is needed, and the RMS of the fiber radius (Eq. S5) was used instead of the arithmetic mean. The fiber volume is approximated by the volume of a cylinder:

$$V = r^2 \pi \cdot l \tag{S1}$$

$$\bar{V} = \frac{1}{n} \cdot \sum_{i=1}^{n} V_i \tag{S2}$$

$$\bar{r}^2 \pi \cdot l = \frac{1}{n} \cdot \sum_{i=1}^{n} r_i{}^2 \pi \cdot l \tag{S3}$$

$$\bar{r}^2 = \frac{1}{n} \cdot \sum_{i=1}^{n} r_i{}^2 \tag{S4}$$

$$\bar{r} = \sqrt{\frac{1}{n} \cdot \sum_{i=1}^{n} r_i{}^2} \tag{S5}$$

Deviation of an equation to predict the fiber diameter

The flow rate Q states which volume of polymer solution V_0 is jetted by the nozzle in a predefined time t.

$$Q = \frac{V_0}{t} \tag{S6}$$

The created fiber volume V_f equals the volume V_T of THV in the jet, given by the volume fraction ϕ_T.

$$\frac{V_f}{t} = Q \cdot \frac{V_T}{V_0} = Q \cdot \phi_T \tag{S7}$$

As the cross section of the fiber is almost circular, the fiber volume is approximated by the volume of a cylinder. Length l_f per time t determines the velocity v_f of the fiber respectively of the jet, since we assume that the speed is constant, when the solvent evaporates and only the diameter reduces.

$$\frac{V_f}{t} = \frac{\left(\frac{d_f}{2}\right)^2 \pi \cdot l_f}{t} = \left(\frac{d_f}{2}\right)^2 \pi \cdot v_f \tag{S8}$$

Combining Eq. S7 and Eq. S8, we achieve an expression to calculate the fiber diameter d_f.

$$\left(\frac{d_f}{2}\right)^2 \pi \cdot v_f = Q \cdot \frac{V_T}{V_0} \tag{S9}$$

$$d_f = \sqrt{\frac{4 \cdot \phi_T \cdot Q}{\pi \cdot v_f}} \tag{S10}$$

For a given concentration and hence, a predefined volume fraction ϕ_T of THV in the polymer solution, the fiber diameter d_f is only depending on the flow rate Q and the fiber velocity v_f.

$$d_f = \underbrace{\left(\frac{4 \cdot \phi_T}{\pi \cdot v_f}\right)^{1/2}}_{C} \cdot Q^{1/2} \tag{S11}$$

$$d_f = \underbrace{\left(\frac{4 \cdot \phi_T \cdot Q}{\pi}\right)^{1/2}}_{B} \cdot v_f^{-1/2} \tag{S12}$$

The velocity of the fiber is caused by the extensional gas flow of the compressed air accelerating the polymer solution inside the nozzle or by the drawing speed of the rotating spool stretching the fiber depending on which one is faster.

A connection between the jet velocity and the pressure difference can be made by Bernoulli's equation. For incompressible flows, the specific energy is constant at any arbitrary point along a stream line.

$$e = \underbrace{\frac{v^2}{2}}_{\substack{specific \\ kinetic \\ energy}} + \underbrace{\frac{p}{\rho}}_{\substack{specific \\ internal \\ energy}} + \underbrace{gz}_{\substack{specific \\ potential \\ energy}} = \text{constant} \qquad \text{(S13)}$$

p: pressure

ρ: density of solution

g: acceleration due to gravity

z: height (z-coordinate)

Two states are distinguished: one inside the nozzle and the other inside the liquid jet.

$$\underbrace{e_n}_{\substack{specific\ energy \\ inside\ nozzle}} = \underbrace{e_j}_{\substack{specific\ energy \\ inside\ jet}} \qquad \text{(S14)}$$

$$\frac{v_n{}^2}{2} + \frac{p_n}{\rho_0} + gz_n = \frac{v_j{}^2}{2} + \frac{p_j}{\rho_0} + gz_j \qquad \text{(S15)}$$

When jetting horizontally, the potential energy is not changing ($z_n = z_j$).

$$\frac{v_n{}^2}{2} + \frac{p_n}{\rho_0} = \frac{v_j{}^2}{2} + \frac{p_j}{\rho_0} \qquad \text{(S16)}$$

$$\frac{p_n}{\rho_0} - \frac{p_j}{\rho_0} = \frac{v_j{}^2}{2} - \frac{v_n{}^2}{2} \qquad \text{(S17)}$$

The velocity inside the nozzle is much smaller than the velocity of the jet.

$$v_n \ll v_j \implies v_j{}^2 - v_n{}^2 \cong v_j{}^2 \qquad \text{(S18)}$$

$$\frac{\Delta p}{\rho_0} = \frac{1}{2} v_j{}^2 \qquad \text{(S19)}$$

$$\Delta p = \frac{1}{2} \rho_0 \cdot v_j{}^2 \qquad \text{(S20)}$$

Δp: pressure difference between nozzle and jet ($\Delta p = p_n - p_j$)

The pressure difference determines the velocity of the jet.

$$v_j = \sqrt{\frac{2 \cdot \Delta p}{\rho_0}} \qquad \text{(S21)}$$

We assume that the polymer solution is accelerated by the pressure difference first, while the density remains constant, and just afterwards, the evaporation of the solvent starts. Also, the loss of kinetic energy owing to viscous dissipation and surface tension is neglected.[1]

Combining Eq. S21 and Eq. S10 gives Eq. S22, which describes the fiber diameter in dependence of the flow rate and the pressure difference applied to the nozzle device.

$$d_f = \left(\frac{8 \cdot \rho_0 \cdot \phi_T{}^2 \cdot Q^2}{\pi^2 \cdot \Delta p}\right)^{1/4} \tag{S22}$$

$$d_f = \underbrace{\left(\frac{8 \cdot \rho_0 \cdot \phi_T{}^2}{\pi^2 \cdot \Delta p}\right)^{1/4}}_{D} \cdot Q^{1/2} \tag{S23}$$

$$d_f = \underbrace{\left(\frac{8 \cdot \rho_0 \cdot \phi_T{}^2 \cdot Q^2}{\pi^2}\right)^{1/4}}_{A} \cdot \Delta p^{-1/4} \tag{S24}$$

Eq. S22 differs just in the term $\sqrt{\phi_T}$ from the Gañán-Calvo equation[1] (Eq. S26) for the jet diameter d_j when using the gas dynamic virtual nozzle-principle.

$$d_f = \sqrt{\phi_T} \cdot \underbrace{\left(\frac{8 \cdot \rho_0}{\pi^2 \cdot \Delta p}\right)^{1/4} \cdot Q^{1/2}}_{\substack{Gañán-Calvo\ equation \\ for\ jet\ diameter\ d_j}} \tag{S25}$$

$$d_j = \left(\frac{8 \cdot \rho_0}{\pi^2 \cdot \Delta p}\right)^{1/4} \cdot Q^{1/2} \tag{S26}$$

The connection between the diameter of the jet and the fiber can also be shown by another simple consideration. The volume of the jet V_j diminishes due to evaporation of acetone.

$$V_f = V_j \cdot \phi_T \tag{S27}$$

$$\left(\frac{d_f}{2}\right)^2 \pi \cdot l_f = \left(\frac{d_j}{2}\right)^2 \pi \cdot l_j \cdot \phi_T \tag{S28}$$

The length of the jet stays constant when the solvent evaporates; just the diameter decreases ($l_f = l_j$).

$$\implies \quad d_f = \sqrt{\phi_T} \cdot d_j \tag{S29}$$

Nozzle deformation during operation

For the calculation of the velocity inside the nozzle, it was necessary to determine the cross-sectional area of the nozzle. The microfluidic channel was cut orthogonally to the flow direction; subsequently, the width n_w and the height n_h of the nozzle were measured by SEM (see Table 1). However, as seen in Fig. S1, the PDMS channels are expanding when a pressure difference or flow rate is applied. The width of the nozzle could be measured during operation by means of an optical microscope. By applying the same expansion coefficient of the nozzle width to the nozzle height, the cross-sectional area during operation could be approximated (1037 µm²).
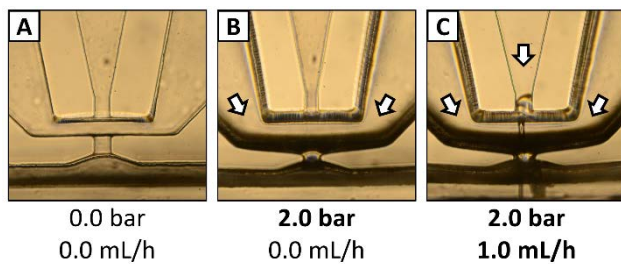
Figure S1: The microchannels of the nozzle are deforming during operation, since the device is made of PDMS elastomer. (A) Idle state, (B) with 2 bar pressure applied, (C) during operation with 1 mL/h and 2 bar.

Influence of working distances between nozzle and spool

The working distance d_s influences the fiber morphology rather than the fiber diameter. The distance d_s between the microfluidic chip and the spool for reeling off was reduced from 8 cm in steps of 1 cm. For a flow rate of 1 mL/h the minimal distance, where a steady fiber with a round cross-sectional shape could be spooled, was 2 cm. At a distance of 1 cm, the fibers fuse and build a network rather than individual fibers (see Fig. S2). Employing the velocity of the jet measured with high-speed cinematography, 3.3 ms are sufficient for the acetone to evaporate from the jetted solution. At flow rates of 2 mL/h and 3 mL/h a distance of 4 cm was needed, which equals a minimal jetting time of 6.5 ms.
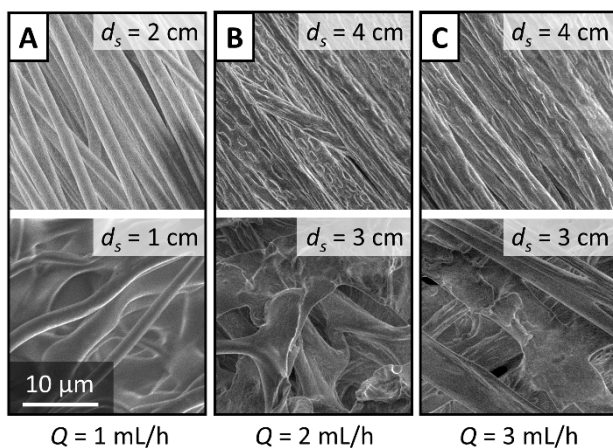

Figure S2: SEM images of bunches of individual fibers (top) and networks of fused fibers (bottom) at different flow rates. The working distance was reduced stepwise until the collected fibers fused into one network. The minimal travel time to form individual fibers could be estimated.

Influence of polymer concentration

The findings of other groups about the influence of polymer concentration on fiber morphology could be confirmed.[2–5] For a solution of a given polymer of a certain molecular weight, a continuous fibrous structure is only obtained above a critical concentration.[2,5] At low polymer concentrations, the formation of beaded fibers is favored.[2] The driving force is the surface tension, which causes oscillations within the jet due to Rayleigh instability.[3,6] Since the viscosity is too low and the chain entanglement density is poor, these oscillations cannot be attenuated.[4] Low surface tension and high evaporation rate would reduce the formation of beads. Higher concentrations also promote the formation of smooth fibers with uniform diameter, as viscoelastic forces retard the deformation of the jet.[3] When the concentration was increased even more, the viscosity got too high to produce fibers by solution blow spinning. Since uniform fibers were desirable for studying the fiber diameter, a reasonable high concentration was used.

Exemplary images for both morphologies can be found in Fig. 5 where the conditions are compared for making beaded and smooth polycaprolactone fibers. The THV fibers showed the same behavior when a solution of less than 20% (w/w) was used. For example, beaded fibers with thin segments of just a few hundred nanometers were obtained at 7–10% (w/w) THV in acetone.

Size distribution of fiber diameter

The uniformity of the fibers is also influenced by varied process parameters. An indicator for the degree of the fluctuation is the standard deviation (SD). Moreover, the relative SD is normalized to the fiber diameter, better illustrating a potential trend since the SD is naturally bigger for thicker fibers.

A close look at Fig. S3 reveals that the size distribution becomes wider when flow rate or drawing speed increases. The histograms confirm this trend which is in accordance to literature.[2] As mentioned before, the solvent needs more time to evaporate from bigger jets, allowing the instabilities to deform the developing fiber in the meantime. An unusually high relative standard deviation was noticed when the pressure difference was quite small being just 1 bar.

A

fiber diameter [µm]

flow rate [mL/h] \ drawing speed [m/s]	5.5	7.7	10.3	12.9	15.5
1.0	2.2	2.0	1.7	1.6	1.6
1.5	2.7	2.2	2.1	1.9	1.8
2.0	3.3	2.5	2.2	2.2	1.9
2.5	3.4	2.7	2.7	2.3	1.9
3.0	3.5	2.8	2.9	2.7	2.0
3.5	4.0	3.3	3.3	2.3	2.7
4.0	4.2	3.4	3.6	2.9	2.7

standard deviation [µm]

flow rate [mL/h] \ drawing speed [m/s]	5.5	7.7	10.3	12.9	15.5
1.0	0.3	0.4	0.3	0.2	0.3
1.5	0.4	0.6	0.4	0.3	0.4
2.0	0.4	0.8	0.4	0.5	0.4
2.5	0.5	0.8	0.8	0.6	0.5
3.0	0.6	0.5	0.8	0.8	0.4
3.5	0.8	0.7	1.1	0.6	0.8
4.0	0.8	0.8	1.3	0.9	0.8

rel. standard deviation [%]

flow rate [mL/h] \ drawing speed [m/s]	5.5	7.7	10.3	12.9	15.5
1.0	12	20	17	15	20
1.5	14	25	20	15	20
2.0	13	30	17	23	23
2.5	14	31	30	27	27
3.0	16	19	29	30	20
3.5	20	20	33	28	29
4.0	18	23	37	31	28

fiber diameter [µm]

flow rate [mL/h] \ pressure [bar]	1.0	1.5	2.0	2.5
1.0	2.3	2.1	2.0	1.9
1.5	2.5	2.6	2.5	2.4
2.0	3.2	3.2	2.7	2.8
2.5	3.4	2.9	3.0	3.1
3.0	3.8	3.6	3.2	3.5

standard deviation [µm]

flow rate [mL/h] \ pressure [bar]	1.0	1.5	2.0	2.5
1.0	1.1	0.4	0.4	0.4
1.5	0.4	0.5	0.5	0.4
2.0	1.5	1.0	0.7	0.4
2.5	0.5	0.5	0.9	0.7
3.0	0.8	0.4	0.6	0.6

rel. standard deviation [%]

flow rate [mL/h] \ pressure [bar]	1.0	1.5	2.0	2.5
1.0	48	19	20	19
1.5	17	19	21	18
2.0	47	31	26	14
2.5	15	18	29	22
3.0	21	12	20	17

B

1.0 mL/h — (1.7 ± 0.3) µm

2.0 mL/h — (2.2 ± 0.4) µm

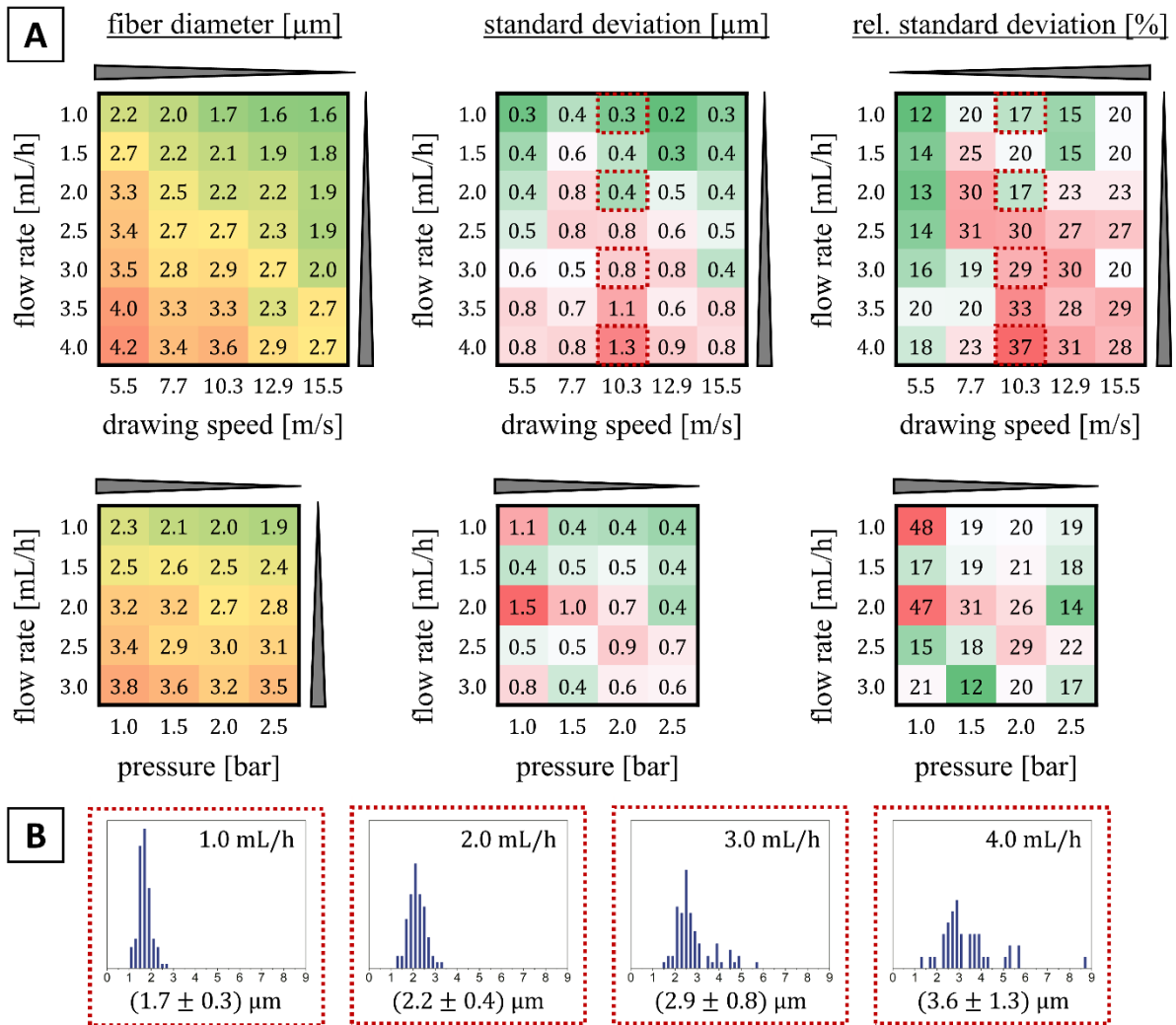3.0 mL/h — (2.9 ± 0.8) µm

4.0 mL/h — (3.6 ± 1.3) µm

Figure S3: (A) Fiber diameter, standard deviation (SD) and relative SD of the THV fiber samples are presented in color-coded tables. Grey wedges indicate assumed trends in the data. (B) Histograms show exemplarily that the size distribution becomes wider when the flow rate increases. The color code only serves as a guide to the eye to visualize the general trends.

Practical guide for solution blow spinning

Microfluidic solution blow spinning may show similar difficulties as electrospinning since both techniques use a thin liquid jet of polymer solution. The following table lists some hints how to solve typical problems.[7]

Table S1: Some typical problems of solution blow spinning and possible adjustments are summarized in this table.

Problem	Possible solution
Spraying / no fiber at all	Increase weight concentration or molecular weight of the polymer
Formation of a beaded chain	Increase weight concentration
Fluctuating fiber diameter	Increase air pressure and decrease flow rate; decrease drawing speed; increase weight concentration; use another solvent with higher vapor pressure
Fusing of fibers / formation of network or film	Increase working distance between nozzle and collection spool; use another solvent with higher vapor pressure
Polymer solution extrudes from the nozzle	Decrease weight concentration of the polymer
Wetting and clogging of nozzle	Incompatible materials; try to switch polymer, solvent or chip to at least one fluorinated component

Literature

1 A. M. Gañán-Calvo, *Phys. Rev. Lett.*, 1998, **80**, 285–288.
2 J. E. Oliveira, E. A. Moraes, R. G. F. Costa, A. S. Afonso, L. H. C. Mattoso, W. J. Orts and E. S. Medeiros, *J. Appl. Polym. Sci.*, 2011, **122**, 3396–3405.
3 H. Fong, I. Chun and D.H. Reneker, *Polymer*, 1999, **40**, 4585–4592.
4 A. Baji, Y.-W. Mai, S.-C. Wong, M. Abtahi and P. Chen, *Composites Science and Technology*, 2010, **70**, 703–718.
5 S. L. Shenoy, W. D. Bates, H. L. Frisch and G. E. Wnek, *Polymer*, 2005, **46**, 3372–3384.
6 Rayleigh, *Proceedings of the London Mathematical Society*, 1878, **s1-10**, 4–13.
7 S. Agarwal, M. Burgard, A. Greiner and J. H. Wendorff, *Electrospinning. A practical guide to nanofibers*, De Gruyter, Berlin, Boston, 2016.